

X rays from atomic systems of combined $Z \simeq 130$ [†]

F. C. Jundt,* H. Kubo,[‡] and H. E. Gove

Nuclear Structure Research Laboratory, University of Rochester, Rochester, New York 14627

(Received 28 May 1974)

The x-ray spectrum in the region from about 2 to 42 keV has been measured for 25-MeV iodine ions incident on thick and thin gold targets, 37.8-MeV gold ions incident on thick tin targets, and 23.9-MeV gold ions incident on thick gold targets. The spectra were obtained for several values of aluminum absorbers inserted between the target and detector. The broad band of x-ray emission lying in energy between about 6.5 and 9.5 keV observed by Mokler *et al.* is confirmed as is their suggestion that it arises from M x rays from the quasiautom system of $Z \simeq 130$. A search for L x rays from these systems was inconclusive.

I. INTRODUCTION

There is considerable current interest in the possibility of observing x rays from quasiautom systems transiently formed when various heavy ions are used to bombard targets of various atomic number, particularly for superheavy quasiautom systems ($Z > 110$). The first report of the observation of x rays from such high-atomic-number systems was made by Mokler *et al.*¹ in 1972. In these experiments, thick targets of Au, Th, and U were bombarded with 10- to 60-MeV iodine ions. In addition to the L and M x rays from the target and the L x rays from the iodine beam, they observed a broad band of x-ray emission lying in energy between the target $L\alpha$ line (approximately 10 keV) and the iodine $L\alpha$ line (approximately 4 keV). They ascribed these x rays to molecular-orbit transitions from the $4f$ to the $3d$ levels in the combined quasiautom. Previous to this work, Saris *et al.*² observed x rays which they ascribed to L x rays from an argon-argon quasiautom ($Z = 36$). In more recent work, Macdonald *et al.*³ have reported the observation of K x rays from a carbon-carbon quasiautom ($Z = 12$) and Meyerhof *et al.*⁴ have observed K x rays from bromine-bromine collisions ($Z = 70$).

In order to verify the results of Mokler *et al.*, the x-ray spectrum has been measured in the energy range from about 2 to 42 keV from 25-MeV iodine ions incident on thick and thin gold targets, from 37.8-MeV gold ions incident on a thick Sn target, and from 23.9-MeV gold ions incident on a thick Au target. Spectra were obtained for several values of aluminum-absorber thickness inserted between the target and detector.

II. EXPERIMENTAL METHOD

The experiments were performed using the model-MP tandem Van de Graaf accelerator in this laboratory. One novel feature involved the use of

a beam of gold ions. The ion source⁵ for such beams consisted of a standard duoplasmatron source producing an intense beam of singly charged positive helium ions, a cesium oven, and a conical gold aperture. Cesium, heated in the oven, coats the conical gold surface which, in turn, is bombarded with the low-energy helium beam. Gold ions are sputtered through the cesium layer and a small but appreciable fraction emerge with negative charge. These are extracted from the source and are appropriately injected into the low-energy end of the tandem. With a terminal voltage of about 5 MV, both charge state 7^+ and 8^+ are relatively abundant from the terminal gas stripper. Gold beams in the energy range 20–40 MeV of intensity up to 100 nA were readily obtained. Iodine beams were obtained by inserting a tube containing iodine crystals in a Penning source.

The momentum-analyzed gold or iodine beams were collimated by high-purity graphite apertures before striking the target. Two blocks of polyethylene interleaved between three permanent magnets placed between the target and the 90° exit window to the detector served to collimate the x rays from the target and to attenuate x rays from scattered beams striking the target-chamber surfaces. The magnets suppressed electrons from the target. The 90° target-chamber exit window was 25- μm -thick beryllium, and a 3.3-mm-diam tantalum collimator was placed between the target-chamber exit window and the entrance window to the detector.

The detector⁶ was a 4-mm-diam 3-mm-thick Si(Li) crystal cooled to liquid-nitrogen temperatures. In this detector, pulsed optical coupling was employed⁶ between the Si(Li) diode and the preamplifier to reduce the usual thermal noise occurring with resistive coupling and to provide dc restoration of the base line. The system also employed pileup rejection.⁶ Data access is inhibited during optical restoration of the base line which

minimizes pileup and gain shift at high counting rates. The resolution was about 180-eV full width at half-maximum for 6.4-keV x rays. An 8.2- μm beryllium window separated the evacuated detector diode from atmosphere.

X-ray spectra were measured for 25-MeV iodine beams incident on a thick gold target with only the two beryllium windows (and an 18-mm path length of air) between the target and detector and with 18 and 38 μm of aluminum absorber inserted. The combined attenuation of the two Be windows (thickness 33 μm) and the 18 mm of air varied from less than 2% for 10-keV x rays to about 23% for 4-keV x rays. Similar measurements were made with a beam of 37.8-MeV gold ions incident on a thick tin target. Tin was chosen because it is the most convenient target material with atomic number close to iodine. The gold-beam energy of 37.8 MeV was chosen because it corresponds to the same distance of closest approach for gold on tin as 25 MeV does for iodine on gold. The same set of measurements were made for 0, 18, and 38 μm of aluminum absorber for 23.9-MeV gold ions on a thick gold target. This energy was chosen because it corresponds to the maximum energy of recoil of gold nuclei when they are struck by 25-MeV iodine ions.

Measurements were also made of the x-ray spectra resulting from 25-MeV iodine bombardment of gold targets of various thicknesses ranging from 10 to 500 $\mu\text{g}/\text{cm}^2$. In these experiments the beam current passing through the target foil was measured in a Faraday cup. Despite the fact that the energy loss of 25-MeV iodine ions in 500 $\mu\text{g}/\text{cm}^2$ of gold is only about 3.5 MeV,⁷ small-angle scattering was sufficiently great that an accurate measurement of beam current could not be made for this thickness of target.

Finally, an attempt was made to measure x rays of energy greater than that of the Au $L\gamma$ x rays (~ 14.2 keV) for both 25-MeV iodine ions on thick gold and 37.8-MeV gold ions on thick tin. A comparison of these two spectra in this region of x-ray energy is of interest with respect to the question of the emission of L x rays from the combined ($Z \approx 130$) quasiatom.

III. EXPERIMENTAL RESULTS

Figures 1–3 show the x-ray spectra measured in the present experiments. In Fig. 1, the results from 25-MeV iodine ions incident on a thick gold target are displayed. Three spectra were measured with 38, 18, and 0 μm of an aluminum absorber between the target and the detector. The prominent features of the spectra are labeled. Figure 2 shows the results for 37.8-MeV gold ions in-

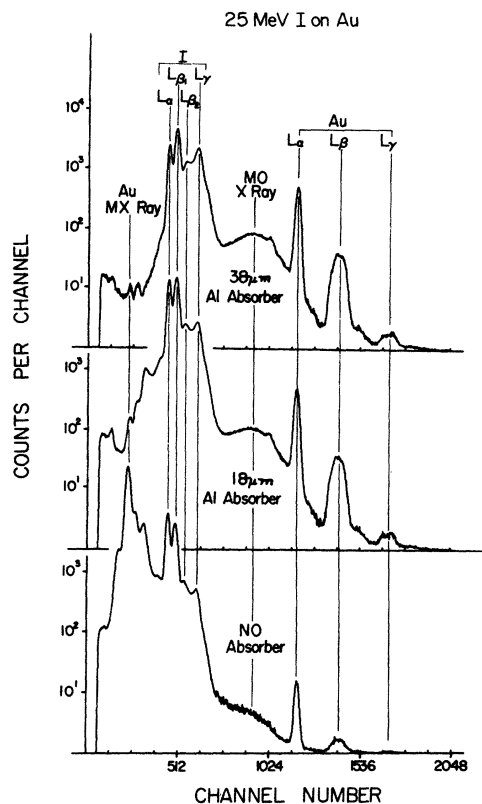


FIG. 1. X-ray spectra from 25-MeV iodine ions incident on a thick gold target for the cases where 38, 18, and 0 μm of aluminum absorber was inserted between the target and detector.

cident on a thick tin target for absorber thickness of 18- and 0- μm aluminum. Because tin has atomic number 50 compared to 53 for iodine, the tin L lines are both lower in energy and have different relative intensity ratios for their components. Figure 3 shows the results for the case where 23.85-MeV gold ions are incident on a thick gold target, again with 38-, 18-, and 0- μm thicknesses of aluminum absorber.

In Fig. 4, the x-ray spectra for 25-MeV iodine ions incident on a thick gold target and 37.8-MeV gold ions incident on a thick tin target are compared. The two spectra have been normalized to the 9.8-keV Au $L\alpha$ line (about channel 1180). As mentioned above, the two energies correspond to the same distance of closest approach for the iodine-gold and gold-tin systems, respectively. The only absorbers between the target and detectors were the two Be windows and 18 mm of air. The gold $L\alpha$, $L\beta$, and $L\gamma$ lines at energies of about 9.8, 11.65, and 14.2 keV, respectively, are prominent features of the upper part of the spectra. The gold $L\gamma$ line at 8.6 keV is also seen weakly. In the lower part of the spectra, the iodine $L\alpha_{1,2}$,

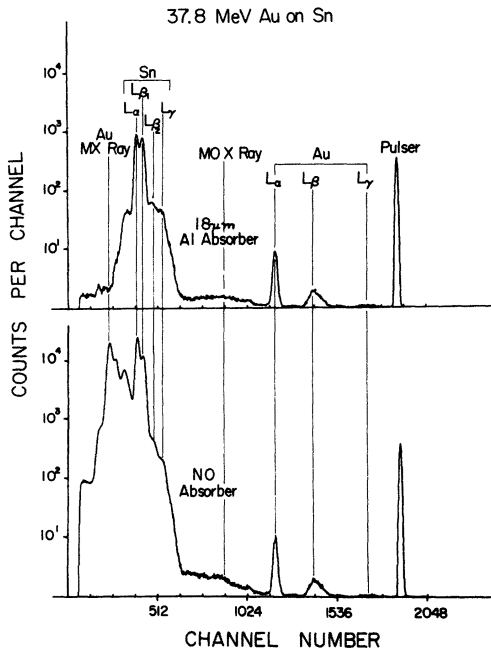


FIG. 2. X-ray spectra from 37.8-MeV gold ions incident on a thick tin target for the cases where 18 and 0 μm of aluminum absorber was inserted between the target and detector.

$L\beta_1$, $L\beta_2$, and $L\gamma_{1,2}$ lines are seen at about 4.1, 4.4, 4.9, and 5.4 keV, respectively (in the gold-on-tin spectra, the equivalent lines from tin at lower energies are seen). In addition, the peaks at lowest energy are various M lines from gold which are seen in both spectra. The broad x-ray distribution lying between the iodine (or tin) L lines and the gold L lines is the feature of the spectra which has been interpreted by Mokler *et al.*¹ as M x-rays from the $Z \approx 130$ quasiatom system. Relative to the gold $L\alpha$ line, it is approximately 30% higher in the iodine-on-gold spectrum than the gold-on-tin spectrum.

Figure 5 shows the same spectra with an 18 μm aluminum absorber between the source and detector. The same features appear as in Fig. 4, except that now there is a 60% or greater difference between the two broad x-ray distributions and the two gold $L\alpha$ lines.

The same data are displayed in a somewhat different fashion in Figs. 6 and 7. Figure 6 shows two curves from the 25-MeV iodine beam on thick gold. The first (shown as open circles) is a portion of the x-ray spectrum between about 4 and 12 keV with 18 μm of aluminum absorber inserted between the target and detector. The second (shown as closed circles) is the ratio of intensity of the spectrum with 18- μm aluminum absorber to that with no aluminum absorber. The ratios of areas under

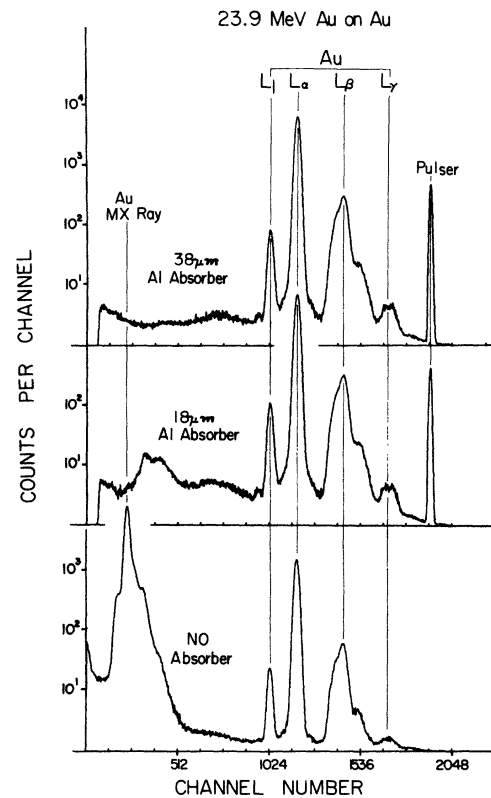


FIG. 3. X-ray spectra from 23.85-MeV gold ions incident on a thick gold target for the cases where 38, 18, and 0 μm of aluminum absorber was inserted between the target and detector.

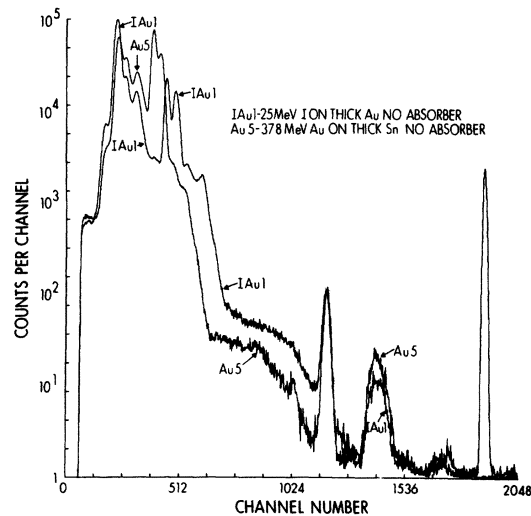


FIG. 4. Spectra of x rays from 25-MeV iodine ions incident on a thick gold target and 37.8-MeV gold ions incident on a thick tin target normalized to the 9.8-keV gold $L\alpha$ line (channel 1180). The only absorber between the target and detector was 33 μm of Be and 18 mm of air.

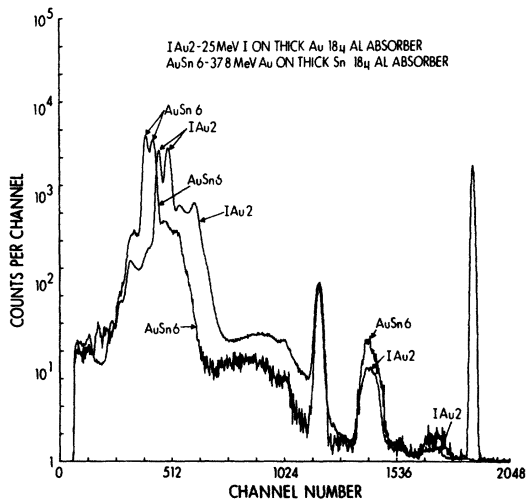


FIG. 5. Same as Fig. 1 with additional absorber consisting of $18\ \mu\text{m}$ of aluminum inserted between the target and detector.

the 9.8-keV gold $L\alpha$ line with and without $18\ \mu\text{m}$ of aluminum absorber has been adjusted to the value of 0.875 corresponding to $\mu/\rho = 28$ for aluminum at this energy.⁸ The dashed line through the intensity ratio or attenuation data is the expected value⁸ for an $18\text{-}\mu\text{m}$ -thick aluminum absorber. The observed attenuation falls below this line in the energy region from about 5.5 to 9.5 keV. It agrees with the expected value for the various L -line peaks of iodine and gold.

In Fig. 7 similar data are plotted for the case of 37.8-MeV gold ions incident on thick tin. Again

the attenuation data are normalized to 0.875 at 9.8 keV. In this case the experimentally measured attenuation falls below the value expected for an aluminum-absorber thickness of $18\ \mu\text{m}$ in the energy range from about 4.6 to 9.0 keV. It should be noted that the strong variation of the measured attenuation across sharp peaks shown here, particularly for the 9.8-keV line, is merely due to a small gain shift between the two spectra.

Figure 8 shows the attenuation data for 25-MeV iodine ions incident on thick gold for an aluminum-absorber thickness of $38\ \mu\text{m}$. In this case, the ratio of areas under the 9.8-keV peak is normalized to the expected value of 0.75. The plotted spectrum is that obtained when the $38\text{-}\mu\text{m}$ aluminum absorber is inserted. The results are similar to those displayed in Fig. 3 except that the attenuation factors are smaller. Again the experimentally observed intensity ratios fall below the expected attenuation curve in the energy region between 5.5 and 9.5 keV.

In order to eliminate the possibility that the broad band of x rays centered at about 8 keV is due to gold ions recoiling in the thick gold target when they are struck by the incident iodine ions, the x-ray spectrum from 23.85-MeV gold ions incident on a thick gold target was measured. This incident energy corresponds to the maximum energy of recoil of gold atoms when bombarded with 25-MeV iodine ions. The three spectra measured with 38-, 18-, and 0- μm thicknesses of aluminum absorber are shown in Fig. 3. A new feature of these spectra is the strong peak corresponding to the gold L_i line which is seen only weakly in the

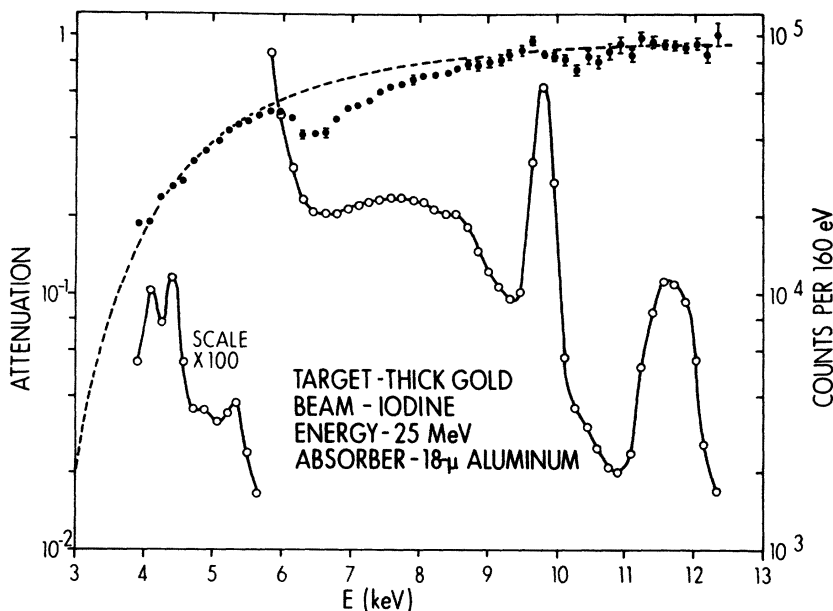


FIG. 6. Lower curve (open circles connected by a solid line), x-ray spectrum for 25-MeV iodine ions incident on a thick gold target with an $18\text{-}\mu\text{m}$ absorber inserted between the target and detector. The right-hand scale giving counts per 160 eV applies to the spectral plot. Closed circles with error bars, ratios of counts in each 160-eV bin of the spectrum with an $18\text{-}\mu\text{m}$ aluminum absorber to that with no aluminum absorber normalized so that the ratio of areas under the gold $L\alpha$ line at 9.8 MeV is 0.875. Dashed curve, expected attenuation ratio for $18\ \mu\text{m}$ of aluminum.

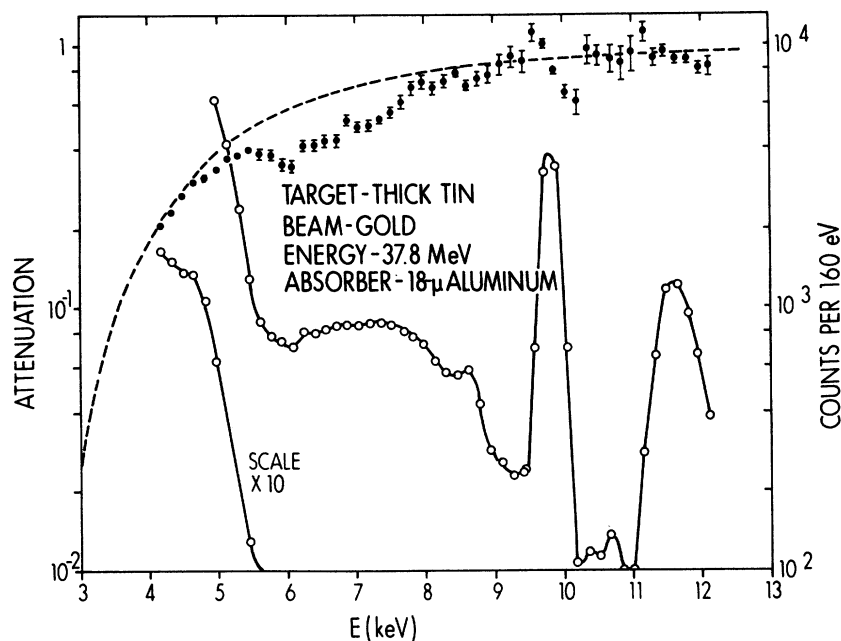


FIG. 7. Same as Fig. 6 for 37.8-MeV gold ions incident on a thick tin target.

iodine-on-gold and gold-on-tin spectra.

Figure 9 compares the x-ray spectra for 25-MeV iodine ions incident on thick gold and 23.85-MeV gold ions incident on thick gold for the case when 38- μ m aluminum absorber is inserted between the target and detector. The two spectra have been normalized to the intensity of the gold $L\alpha$ line. Clearly, gold recoils are contributing negligibly to the broad x-ray band centered at 8 keV observed in the iodine-on-gold spectrum.

The attenuation data for the gold ions incident on

a thick gold target is shown in Fig. 10. These curves are similar to those of Figs. 6-8. The solid curve connecting open circles is the x-ray spectrum from 23.9-MeV gold ions incident on a thick gold target with 18- μ m-thick aluminum foil inserted between the target and detector. The closed circles are the ratio of the intensity of the spectrum with an 18- μ m aluminum absorber to that with no aluminum absorber. Again the ratio of areas under the 9.8-keV gold $L\alpha$ line has been adjusted to the value 0.875 expected⁸ for this thick-

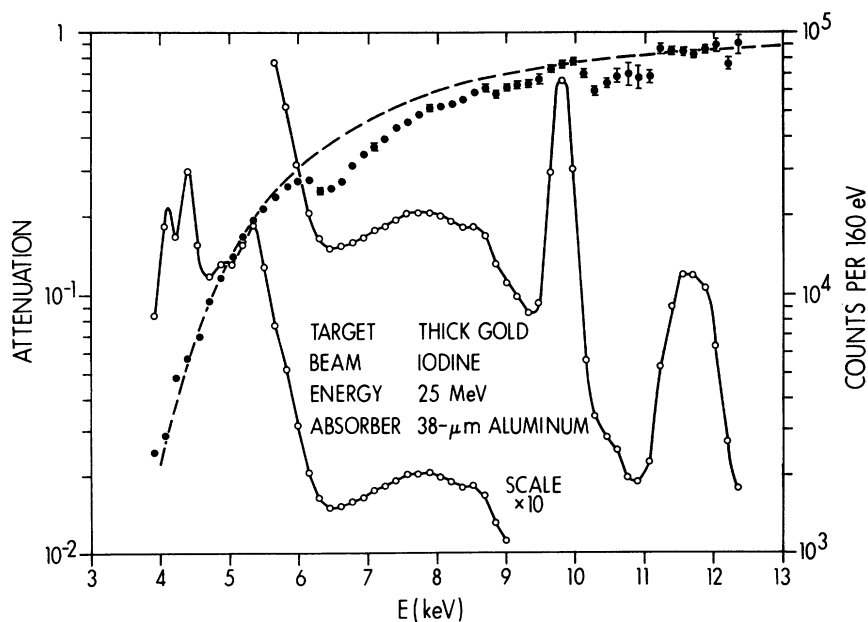


FIG. 8. Same as Fig. 6 for 25-MeV iodine ions incident on a thick gold target except that a 38- μ m aluminum absorber was used. For the attenuation data, the ratio of the areas under the 9.8-keV peak was normalized to the expected value of 0.75.

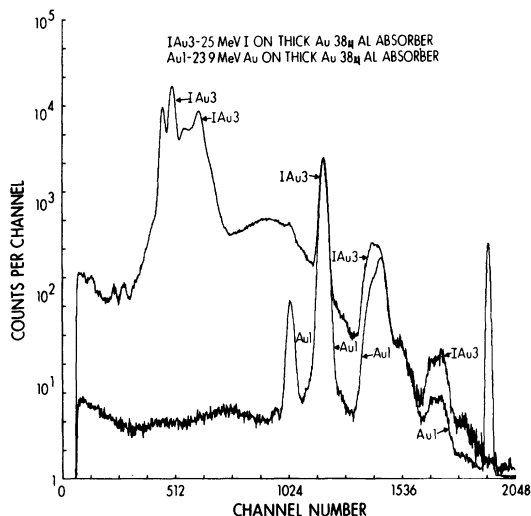


FIG. 9. Spectra of x rays from 25-MeV iodine ions incident on a thick gold target and 23.85-MeV gold ions incident on a thick gold target normalized to the 9.8-keV gold $L\alpha$ line. A 38- μ m aluminum absorber was inserted between target and detector.

ness of absorber. The dashed curve again is the expected attenuation ratio. Unlike the previous plots of this kind shown in Figs. 6–8, the measured attenuation ratio lies above the expected value for all energies between 3.5 and 9.5 keV.

In order to determine whether the general shape of the spectrum resulting from 25-MeV iodine ions incident on gold (shown in Fig. 1) was dependent

on target thickness, the spectra were measured for gold-target thicknesses of 10-, 30-, 50-, 100-, and 500- $\mu\text{g}/\text{cm}^2$ gold evaporated on 40 $\mu\text{g}/\text{cm}^2$ carbon backings. Such variations in spectral shape could result from processes having different dependences on beam energy or from processes depending on single versus multiple collisions. The beam current was measured in a Faraday cup biased to eliminate secondary electrons. The energy loss in gold for 25-MeV iodine ions is 6.42 MeV (mg cm^2).⁷ For the thickest target employed (500 $\mu\text{g}/\text{cm}^2$) it was found that the current reading was unreliable (presumably owing to small-angle scatter). The accuracy with which the various target thicknesses were known was estimated to be about $\pm 5 \mu\text{g}/\text{cm}^2$. A spectrum was also measured for 25-MeV iodine ions incident on a 40- $\mu\text{g}/\text{cm}^2$ carbon foil so that corrections for the target backing could be made. The results are summarized in Fig. 11. The inset in Fig. 11 shows the counts due to L x rays from iodine divided by the beam charge and target thickness (R_3) plotted as a function of target thickness. The error bars indicate the principal uncertainty in the measurement—that of target thickness. The main graph shows two curves. The closed circles are the ratio of the counts in the gold $L\alpha$ line to the iodine L lines (R_2), and the open circles are the ratio of the counts in the broad x-ray band centered at 8 keV to the iodine L lines (R_1) as a function of target thickness.

These ratios have been corrected for x-ray self-absorption to take into account the fact that the absorption coefficient for iodine L x rays (~ 4.2

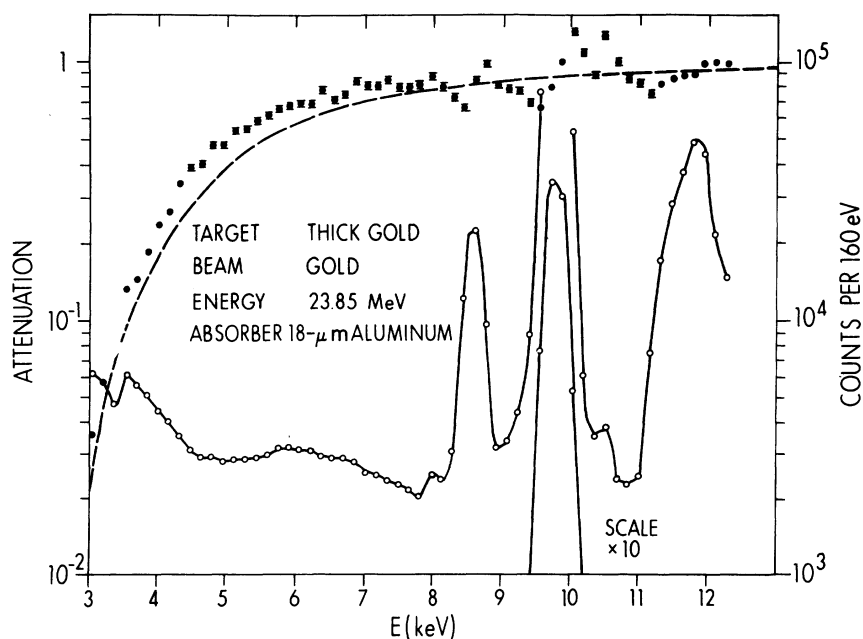


FIG. 10. Same as Fig. 6 for 23.85-MeV gold ions incident on a thick gold target.

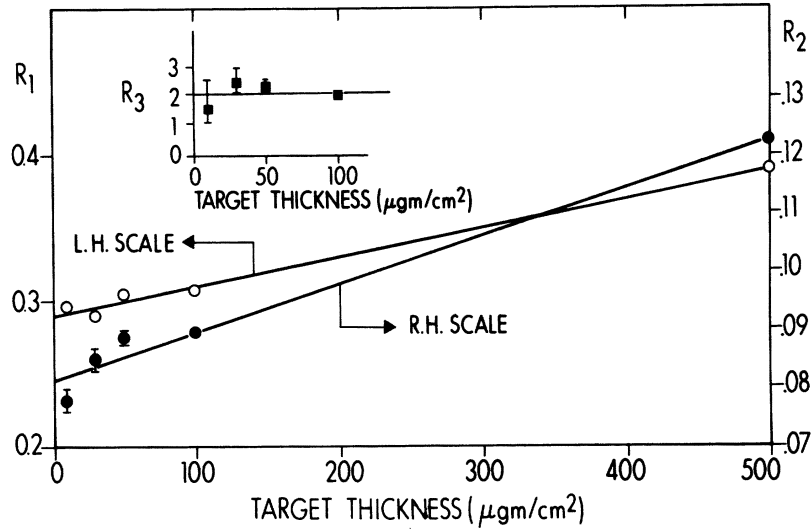


FIG. 11. Yields and ratio of yields of various regions of the x-ray spectrum resulting from 25-MeV iodine ions incident on a gold target as a function of target thickness. The inset plots the intensity of the iodine L lines divided by total beam charge and target thickness (R_3) against target thickness (closed squares). The main graph shows the ratio of counts in the gold $L\alpha$ peak (R_2 , closed circles, right-hand scale) and the counts in the broad x-ray band centered at 8 keV (R_1 , open circles, left-hand scale) to the counts in the iodine L lines as a function of target thickness. An 18- μm -thick aluminum absorber was inserted between the target and the detector.

keV) is about ten times as great as for gold L x rays (~ 9.8 keV) in the gold target. In calculating these self-absorption corrections, it was assumed that the cross section for production of x rays throughout the energy spectrum is relatively constant as a function of beam energy over the range covered by energy loss in the target (i.e., 25–22 MeV for the 500- $\mu\text{g}/\text{cm}^2$ -thick target). The experimental uncertainties in these two ratios, unless indicated, are smaller than the diameter of the points and are statistical in nature. To within the experimental uncertainties, the yield of iodine L x rays is proportional to target thickness, while that of the gold $L\alpha$ line and the broad 8-keV line increases more rapidly than linearly with target thickness.

As part of these thin-target-yield measurements, the absolute cross section was obtained. The beam current was measured in a biased Faraday cup, and it was assumed that 25-MeV iodine ions have a mean charge state⁹ of about 14 after passing through a 100- $\mu\text{g}/\text{cm}^2$ gold foil. In the region of the spectrum from 6.3 to 9.4 keV, the measured cross section was about 100 b (or approximately 32 b/keV). This is to be compared with the value of 64 b/keV obtained by Stein.¹⁰

An attempt was made to detect possible L x rays from the combined gold-tin system. The maximum energy of such radiation is expected to be about 30 keV, which is close to the $K\alpha$ and $K\beta$ x-ray energies of approximately 25.2 and 28.5 keV, respectively, from tin. A comparison was

made between two spectra in the x-ray energy region from 5 to 45 keV. In the first case, a thick gold target was bombarded with 25-MeV iodine ions, and in the second, a thick tin target was bombarded with 37.8-MeV gold ions. Because vacancies in the gold L shell are required in order for the quasiautomic L x rays from the combined system to occur, one would expect to produce such x rays with higher probability when gold is employed as the projectile rather than the target. In the energy region from 22 to 42 keV, the observed intensity from gold on tin was about 8 ± 1 times that from iodine on gold relative to the Au $L\alpha$ line. Although this is a significant difference and suggests that quasiautomic L x rays are, in fact, being observed, there are a number of residual uncertainties discussed in Sec. IV which need further experimental investigation before definite conclusions can be drawn.

IV. DISCUSSION

The broad band of counts centered at 8 keV in the x-ray spectrum was observed by Mokler et al.¹ and also observed in the present work when iodine ions of various energies are incident on thick gold targets and when 37.8-MeV gold ions are incident on a thick tin target. This band could arise from causes other than the quasiautomic mechanism proposed by Mokler. These are (i) pulse pileup effects due to finite electronic resolving time and high counting rates of low-energy x rays; (ii) target

impurities; (iii) interactions between recoiling and stationary target atoms; (iv) combination of low-energy tails of intense higher monoenergetic gold L x rays and high-energy tails of intense lower monoenergetic iodine or tin L x rays; and (v) electron bremsstrahlung, nuclear bremsstrahlung, or radiative electron capture. The present experiments were designed to eliminate these possibilities.

Pileup effects are rendered negligible as a result of the pileup rejection⁶ employed in the detector circuitry. From the known counting rates in the region of the spectrum corresponding to iodine L x rays (4.02–5.30 keV), the pileup contribution to the region of energy encompassing the broad peak (6.5–9.5 keV) in the 25-MeV iodine on thick gold runs (Fig. 1) was 5%, 0.2%, and 0.2%, respectively, for the three cases of no absorber, 18- μ m aluminum absorber, and 38- μ m aluminum absorber, respectively. This assumes a 1- μ sec pileup rejection time, which is probably an upper limit. It should be noted that when absorbers were inserted, the beam current was increased to give higher counting rates in the 8-keV region, so the expected quadratic dependence of pileup on counting rate does not apply.

The possibility that the 8-keV band is due to target impurities is immediately eliminated by essentially reversing the role of target and projectile as done in the present experiments—unless, of course, the same impurity happened to be present in both the thick gold and thick tin targets which is unlikely. In any case, impurities would give rise to lines in the spectrum, not to broad bands. Figures 4 and 5 show that the spectra for the two experiments are very similar. The fact that when the two spectra (iodine ions on a thick gold target and gold ions on a thick tin target) are normalized to the gold $L\alpha$ line, the broad x-ray band at 8 keV is about 30% greater for iodine on gold than gold on tin when no aluminum absorber is inserted and about 60% greater when an 18- μ m-thick aluminum absorber is inserted can be attributed to the effects of the high-energy tails of the intense L lines from iodine and tin. Because the iodine L lines are higher in energy, they contribute more counts under the broad peak than the tin L lines. This difference is enhanced when an aluminum absorber is added because this selectively absorbs more of the tin L line. It could also be due to a difference in the fluorescent yield of the gold $L\alpha$ line depending on whether gold is the projectile or the target since, in the former case, the radiating gold ion is more highly ionized. Since one might expect the fluorescent yield to increase with increased ionization, normalizing the iodine-on-gold and gold-on-tin spectra to the

gold $L\alpha$ line would make the 8-keV band appear less intense when gold is the projectile than when it is the target as observed. It could also, in part, be due to the fact that the proposed molecular-orbit mechanism is different when the role of target and projectile is interchanged. Both these latter effects, of course, would be independent of the absorber thickness. Finally, the fact that the intensity of the broad 8-keV band increases faster than linearly with respect to the iodine L lines as the target thickness is increased also precludes the possibility that it arises from a target contaminant.

In order to completely eliminate the possibility that this broad 8-keV distribution, in the case of iodine ions incident on gold, is not associated with gold ions recoiling in gold (although this possibility is also eliminated by reversing the role of target and projectile), thick gold targets were bombarded with gold beams of energy 23.9 MeV. This energy is equal to the maximum gold recoil energy from 25-MeV iodine ions incident on gold. The results are shown in Fig. 3, and a comparison between the iodine-on-gold and gold-on-gold spectra is shown in Fig. 9, with the two spectra again normalized to the gold $L\alpha$ line. Clearly the gold recoil contribution to the broad 8-keV peak is negligible. Significant differences are apparent in the gold L lines observed in the two cases. These differences deserve further detailed study, but were not pursued in the work reported here.

A detailed analysis has been carried out on the spectra obtained with different thicknesses of absorber inserted between the target and detector. The results are shown in Figs. 6–8 and 10. For both the case of iodine incident on thick gold (Figs. 6 and 8) and gold incident on thick tin (Fig. 7) the region of the spectrum between 6 and 9 keV contains pulses due to x rays of lower energy (and perhaps also of higher energy), whereas for gold on gold (Fig. 10) the spectrum below 8 keV must contain appreciable contributions from the tails of the higher-energy gold L lines. For the iodine-gold and gold-tin combinations, the question is whether such high and low tails of lower- and higher-energy x rays can completely account for the pulses observed in the spectrum in this region of energy centered at about 8 keV.

In an attempt to answer this question, an analysis was made of the spectrum shown in Fig. 8. The portion of this spectrum between about 5.5 and 12.5 keV was plotted linearly and is shown in Fig. 12. A plausible high-energy tail was drawn, the intensity of which was assumed to be entirely due to 5.65-keV x rays, and a low-energy tail was constructed, the intensity of which was assumed to be entirely due to 9.8-keV x rays. The energy of

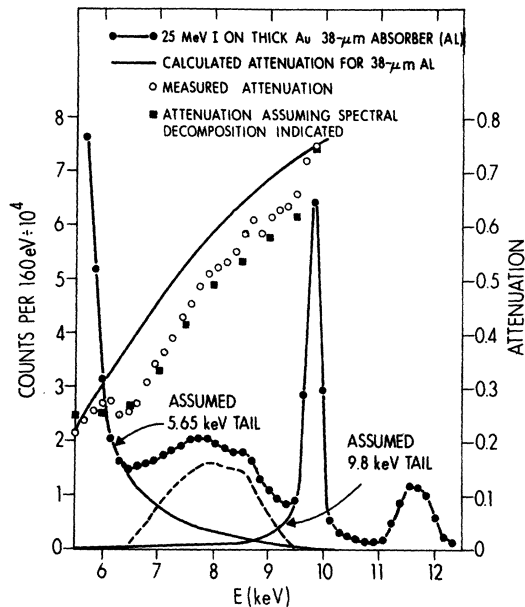


FIG. 12. Linear plot of the x-ray spectrum from 25-MeV iodine ions incident on a thick gold target with 38 μm of aluminum absorber between the target and detector. Plausible high-energy tails on the iodine L x rays and low-energy tails on the gold $L\alpha$ x rays are shown. The expected attenuation using this spectral decomposition (closed squares) is compared with the measured attenuation (open circles).

5.65 keV is higher than the highest L line from iodine ($L\gamma_2$), which has an energy of about 5.4 keV. It corresponds, however, to a slight shoulder on the high-energy side of the iodine L spectrum (see, for example, Fig. 8) and is most likely due to x rays from radiative electron capture, as discussed below. The difference between these assumed tails and the measured spectrum is shown as a broad dashed peak. No acceptable combination of high and low tails can be constructed to eliminate this peak. Furthermore, the attenuation of such a composite spectrum when 38 μm of aluminum absorber is inserted (shown as the closed squares in Fig. 12) agrees reasonably well with the measured attenuation (shown as open circles) and differs appropriately from the calculated attenuation (shown as the solid line). Thus, there is no question that a broad band of x radiation centered at 8 keV is observed when iodine ions are incident on gold (and when gold ions are incident on tin). Furthermore, it is interesting to note that the shape of this broad band cannot differ substantially from that shown by the dashed line in Fig. 12. In particular, it must be almost zero at some energy between 6 and 7 keV (and inferentially at all energies below this as well) or the observed attenuation in this region would not be ac-

curately reproduced.

Finally, the question remains as to whether there are known interaction mechanisms which could produce this broad band of radiation for the iodine-gold and gold-tin systems other than that proposed by Mokler *et al.*¹ Such mechanisms would include electron bremsstrahlung, nuclear bremsstrahlung, and radiative electron capture.

The first possibility can be eliminated in part because the maximum energy of the electron-bremsstrahlung spectrum corresponds to the maximum energy imparted to an unbound electron by a head-on collision between the incident heavy ions (iodine, for example) and an electron at rest. For 25-MeV iodine ions, this corresponds to 0.4 keV.

Beyond this upper limit on the bremsstrahlung energy owing to iodine collisions with unbound electrons, however, there will be a monotonically decreasing contribution to the bremsstrahlung spectrum from collisions involving bound electrons. This phenomenon has been investigated recently for protons in the MeV range by Folkmann *et al.*¹¹ in connection with their work on trace-element analysis. In these studies it was found that the ultimate limitation on the sensitivity for detection of trace elements from their characteristic x-ray emission under proton bombardment was due to the bremsstrahlung spectrum from electrons ejected by the bombardment from bound orbits in the atoms constituting the matrix of the sample. Folkmann¹² has carried out a preliminary calculation for the case of 25-MeV iodine ions incident on gold. In this calculation he has assumed a binary encounter or plane-wave Born approximation, although he states that the validity of this approximation is uncertain for such low-energy heavy ions. The advantage of the approximation, however, is that a simple scaling relation can be employed which relates the cross section for production of secondary electrons in the target for a projectile characterized by Z_1 , A_1 , and E_1 to that for incident protons on the same target of energy E_1/A_1 . This relation states that the cross section for the former is a factor of Z_1^2 higher than for the latter. He finds that the largest contribution to secondary electrons whose energies lie in the region from 4 to 10 keV arises from those ejected from the gold M and N shells when gold is bombarded with 0.197-MeV protons ($E_1/A_1 = 25/127 = 0.197$ MeV). The total bremsstrahlung cross section in the region from 6.3 to 9.4 keV from all bound electrons ejected from gold atoms when bombarded with 25-MeV iodine ions calculated in this way (including the Z_1^2 factor) is approximately 72 mb. In the corresponding energy region, the results presented here yield a cross section of approximately 100 b.

In addition, of course, one must consider the bremsstrahlung due to bound electrons ejected from the M and N shells of the incident iodine atoms by the gold-target nuclei. This is equivalent to 38.8-MeV gold ions incident on iodine and $E_1/A_1 = 0.197$ MeV as before. The cross section will be higher for this process by a factor of about 2 because of the Z_1^2 factor and will also differ because of the different electron binding energies involved. The cross section for this was not calculated, but it is highly unlikely that including it can account for the observed cross section of 100 b.

In the case of nuclear bremsstrahlung, the maximum bremsstrahlung energy corresponds to the maximum heavy-ion energy, so the spectrum includes the region of interest around 8 keV. It is therefore again necessary to compare the measured absolute cross section in this region of the spectrum with that predicted for nuclear bremsstrahlung. An expression for the latter has been given by Alder *et al.*¹³ for dipole radiation. For an energy interval of 3 keV centered at 8 keV, this expression yields a cross section of about 10^{-3} b for 25-MeV iodine ions. As discussed above, the cross section measured in the present experiments (again for a 3-keV energy interval centered at 8 keV) is approximately 100 b. Nuclear bremsstrahlung is thus five orders of magnitude lower in cross section and cannot account for the observed 8-keV band.

Radiative electron capture (REC) is a process in which electrons approximately at rest in the target are captured into, in this case, an L -shell vacancy in the moving incident iodine atom. The energy of the radiation emitted in this process is the binding energy of an electron in the appropriate L shell (i.e., $2s_{1/2}$, $2p_{1/2}$, or $2p_{3/2}$) for the particular charge state of the ion at the time the electron capture takes place plus the kinetic energy of the electron relative to the moving ion. For 25-MeV iodine ions, the latter amounts to only 107 eV. The L -shell binding energy depends on the number of electrons which have been stripped from the moving ion and the orbits in which the remaining electrons are distributed. A reasonable estimate of the average charge state of 25-MeV iodine ions in a solid target, which can be obtained from the review article of Betz,⁹ is $\bar{q} = 14$ (this is the value that was used above to calculate the absolute cross section). The binding energies of L -shell electrons have been calculated¹⁴ using the Hartree-Fock-Slater method and including relativistic and spin-orbit corrections according to the prescription of Herman and Skillman.¹⁵ For a single electron vacancy in the $2s$ shell or the $2p$ shell or both, with the remaining vacancies distributed among the $4d$, $5s$, and $5p$, shells, the maximum L -shell

binding energy is about 5.7 keV, which would correspond to an REC energy of 5.8 keV including the kinetic-energy term. Values of binding energy up to 6.5 keV are indicated for two vacancies in the $2s$ shell, but this is clearly unlikely to occur. Vacancies in the $1s$ shell are of negligible probability since no iodine K x rays are observed (the K fluorescent yield for iodine is about 0.9). The L -shell binding energy is relatively independent of the vacancy distribution in the outer shells. It thus appears that the REC peak would be at about 5.8 keV, which is substantially below the approximate 8-keV centroid observed for the broad band. As noted above, a slight shoulder is observed on the high-energy side of the iodine L spectrum (Fig. 8) at an energy of approximately 5.65 keV, and this is most likely the REC contribution. Finally, it should be recalled that in the work of Mokler *et al.*¹ the centroid of the broad band occurs at 8, 9.5, and 10 keV, respectively, for iodine ions incident on Au, Th, and U. The spectral-distribution REC radiation would be essentially independent of target Z .

Having exhausted all the known possible alternative explanations for the broad 8-keV radiation band, one is led to the conclusion that the explanation originally advanced by Mokler *et al.* is correct, namely, that it arises from M x-ray transitions in the $Z \approx 130$ quasiautom transiently formed in the present work when iodine ions are incident on gold (or gold ions incident on tin). It should be noted that the quasiautom transitions involved differ when the role of projectile and target is reversed, as will be discussed below.

There remains, however, one puzzle connected with one of the experiments reported here. It has been pointed out by Stein¹⁰ that one would not expect the ratio of the Au $L\alpha$ line and the broad 8-keV band to continue rising with respect to the L lines for target thicknesses much beyond a few $\mu\text{g}/\text{cm}^2$ —certainly not up to thicknesses as great as $500 \mu\text{g}/\text{cm}^2$ as observed here (Fig. 11). He argues that since the production of both Au L radiation and the 8-keV band depends on the existence of a beam of iodine ions containing L vacancies, one expects a variation with target thickness for these two processes compared to that for the iodine L x rays of the form $1 - e^{-t/\tau}$, where t is the time taken for the iodine beam to pass through a given target thickness and τ is the lifetime of the L vacancy in iodine. If the latter is taken to be 2×10^{-16} sec, the $1 - 1/e$ thickness for 25-MeV iodine ions is $2.5 \mu\text{g}/\text{cm}^2$. For the yield ratio to continue to increase up to target thicknesses of $500 \mu\text{g}/\text{cm}^2$ implies that the L -vacancy lifetime in iodine is about a factor of 100 longer than the value assumed by Stein when as many as 14 elec-

trons have been removed. This seems unlikely, but no detailed explanation for the results displayed in Fig. 11 is presently available. It should be emphasized that one might be inclined to ascribe this particular feature of the data to some unknown experimental error were it not for the fact that one is comparing ratios of intensities of various regions in an individual spectrum measured for one target thickness to those same ratios measured in another spectrum for a different target thickness, and it is difficult to invent plausible reasons for error. The spectra literally change their shape as the target thickness is increased from 10 to 500 $\mu\text{g}/\text{cm}^2$.

Turning now to the attempt to observe L x rays from the $Z \approx 130$ quasiatom systems under discussion here, the results described above showed that the intensity observed in the spectrum in the region of 30 keV (the expected energy of such quasiatom L x rays) relative to the Au $L\alpha$ line was approximately an order of magnitude higher for gold ions incident on tin than for iodine ions incident on gold. In neither case was there any evidence for characteristic tin or iodine K x rays which would also occur in this region of energy. This enhanced intensity is what one might expect for quasiatom L x rays because vacancies in the gold L shell which can be carried by the gold projectile into a second collision are a prerequisite for the production of such quasiatom L x rays. There are, however, two other reasons why one might expect to observe more counts above the Au L lines for gold on tin as opposed to iodine on gold relative to the Au $L\alpha$ line. In the first place, the Au $L\beta$ and $L\gamma$ lines are less intense relative to the $L\alpha$ line for iodine incident on gold, as can be seen from Fig. 5; hence the contribution from high-energy tails of these lines will make less of a contribution. Second, there is the possibility that the Compton tail from 77-keV γ rays arising from the Coulomb excitation of the first excited state in ^{197}Au contributes counts to this region of energy. The cross section for this reaction is exceedingly small, however, at the energies involved, but a rough estimate indicates that it is a factor of 2 higher for 37.8-MeV gold ions incident on a thick tin target than it is for 25-MeV iodine ions incident on thick gold. Since both effects are in the direction of increasing the counts in the region of energy where one expects the quasiatomic L band to occur for gold on tin over that for iodine on gold, the observation of increased counts is not, at present, conclusive evidence that such x rays are observed.

The mechanism suggested by Mokler *et al.*¹ to explain the broad 8-keV band is based on the molecular-orbit-level diagram proposed by Fano and

Lichten¹⁶ and developed by Lichten.¹⁷ A highly simplified version of the diagram exhibited by Mokler *et al.*¹ for the iodine-gold system is shown in Fig. 13. It contrasts the mechanism for producing Au L x rays and quasiatom M x rays for the case of iodine incident on gold and gold incident on iodine (tin in the present work).

For the case when iodine is the projectile and gold the target the suggested explanation is as follows.

(i) The gold M lines arise from a single collision promoting an electron into the continuum via the strongly rising $3d$ level in gold. This occurs in a single collision.

(ii) The iodine L lines also occur as a result of a single collision in which electrons in the $2p$ orbit of iodine are promoted via the $4f$ quasiatom level to a region where they are readily ionized. On separation, these vacancies can be transferred back to all levels in the iodine L shell.

(iii) Two collisions are required to produce the gold-target L x rays. The vacancy in the iodine $2p$ level created in the first collision as described above may still exist when a second collision occurs. It can then be transferred via the $3d$ united atom levels to the $2p$ level in the separated gold target. L x rays from gold are then emitted as shown by the vertical arrow on the right-hand side of the figure.

(iv) This same two-step mechanism can also give rise to the quasiatom x ray transitions. In

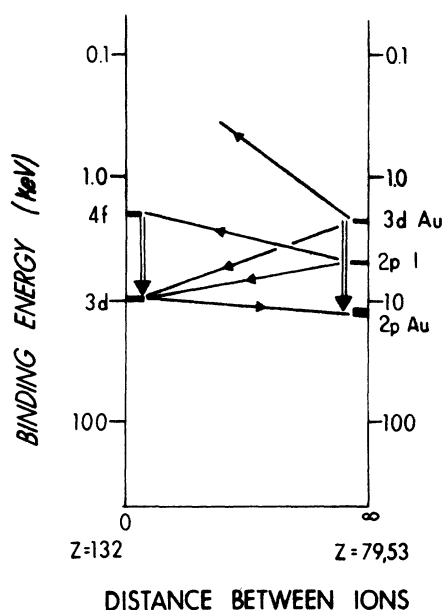


FIG. 13. Highly simplified molecular-orbit diagram for the iodine plus gold system showing the level shifts and transitions observed in the present experiments.

particular, the $4f$ to $3d$ transition shown by the vertical arrow on the left-hand side of the diagram can occur during the second collision before the vacancy in the incident-iodine-ion L shell can be transferred to the gold-target L shell.

The question then arises as to what mechanism applies when the role of target and projectile are reversed. Obviously both one-step processes discussed above are independent of which is the projectile and which the target. Clearly the production of gold L x rays when gold is the projectile cannot be a two-collision process involving the production of holes in the iodine-target L shell in the first collision. Referring again to Fig. 13, the following is a possible mechanism. In the first collision, a hole in the $3d$ shell in gold is created by the sharply rising $3d$ level in gold. This vacancy can then be transferred to the $2p$ shell in gold in the second collision via the $3d$ level in the combined atom. This same mechanism can give rise to the quasiautom x rays. This is the first example in which this particular mechanism occurs. Since in both target-projectile situations the same process gives rise to both the gold $L\alpha$ lines and the molecular-orbital x rays, although the atomic and molecular orbits involved differ depending on

which is the projectile and which the target, one expects the ratio to be almost the same—as it is.

V. CONCLUSIONS

A number of experiments involving gold and iodine projectiles and gold and tin targets have been carried out which verify the conclusion of Mokler *et al.*¹ that the broad band of radiation centered at about 8 keV when the combined Z of the projectile-target system is about 130 arises from M x rays of the quasiautom system.

ACKNOWLEDGMENTS

The authors wish to acknowledge informative discussions with R. Liebert, P. Armbruster, and H. J. Stein. They also express their appreciation to R. Liebert for calculating the iodine L orbit radiative-electron-capture energies for the case when 14 electrons have been removed from various electron orbits in iodine. They are also grateful to F. Folkmann for performing calculations of the bremsstrahlung spectrum due to the ejection of bound electrons from gold under 25-MeV iodine bombardment.

[†]Work supported by the National Science Foundation.

*On leave from Laboratoire de Physique Nucléaire et d'Instrumentation Nucléaire, Centre de Recherches Nucléaires, Strasbourg, France.

[‡]Present address: School of Medicine, Kitasato University, Sagami, Kanagawa, Japan, 228.

¹P. H. Mokler, H. J. Stein, and P. Armbruster, *Phys. Rev. Lett.* **29**, 827 (1972).

²F. W. Saris, W. F. van der Weg, and H. Tawara, *Phys. Rev. Lett.* **28**, 717 (1972); F. W. Saris, I. V. Mitchell, D. C. Santry, J. A. Davies, and R. Laubert, in *Proceedings of the International Conference on Inner-Shell Ionization Phenomena, Atlanta, Georgia, 1972*, edited by R. W. Fink, J. T. Manson, I. M. Pálms, and R. V. Rao (U.S. AEC, Oak Ridge, Tenn., 1973), p. 1255.

³J. R. Macdonald, M. D. Brown, and T. Chiao, *Phys. Rev. Lett.* **30**, 471 (1973).

⁴W. E. Meyerhof, T. K. Saylor, S. M. Lazarus, W. A. Little, B. B. Triplett, and L. F. Chase, Jr., *Phys. Rev. Lett.* **30**, 1279 (1973).

⁵Designed by K. H. Purser.

⁶Manufactured by Princeton Gamma-Tech Incorporated, Princeton, N. J.

⁷L. C. Northcliffe and R. F. Schilling, *Nucl. Data A* **7**, 233 (1970).

⁸W. C. Veigele, E. Briggs, L. Bates, E. M. Henry, and B. Bracewell, Kaman Sciences Report No. DNA2433F, Vol. I, Rev. I, KN-71-431(R), Colorado Springs, Colo. 80907.

⁹H. D. Betz, *Rev. Mod. Phys.* **44**, 465 (1972) [Eq. (5.8)].

¹⁰H. J. Stein (private communication).

¹¹F. Folkmann, C. Gaarde, T. Huus, and K. Kemp, *Nucl. Instrum. Methods* **116**, 487 (1974).

¹²F. Folkmann (private communication).

¹³K. Alder, A. Bohr, T. Huus, B. Mottelson, and A. Winther, *Rev. Mod. Phys.* **26**, 432 (1956).

¹⁴R. Liebert (private communication).

¹⁵F. Herman and S. Skillman, *Atomic Structure Calculations* (Prentice-Hall, Englewood Cliffs, N.J., 1963).

¹⁶U. Fano and W. Lichten, *Phys. Rev. Lett.* **14**, 627 (1965).

¹⁷W. Lichten, *Phys. Rev.* **164**, 131 (1967); M. Barat and W. Lichten, *Phys. Rev. A* **6**, 211 (1972).